2006

A qualitative analysis on nonconstant graininess of the adaptive grids via time scales

Paul W. Eloe
University of Dayton, peloe1@udayton.edu

Stefan Hilger
Katholische Universität Eichstätt

Qin Sheng
University of Dayton

ROCKY MOUNTAIN
JOURNAL OF MATHEMATICS
Volume 36, Number 1, 2006

A QUALITATIVE ANALYSIS ON NONCONSTANT GRAININESS OF THE ADAPTIVE GRIDS VIA TIME SCALES

P.W. ELOE, S. HILGER AND Q. SHENG

ABSTRACT. Calculus on time scales plays a crucial role in unifying the continuous and discrete calculus. In this paper, we apply the time scales calculus methods to study qualitatively properties of the numerical solution of second order ordinary differential equations via different finite difference schemes. The properties become particularly interesting in the case when the computational grids are nonuniform, on which the finite difference operators do not commute. To investigate the solution properties, we introduce the graininess function, and express the numerical solution as functions of the variable grid steps, that is, functions of the graininess and its dynamic derivatives implemented by using the time scales analysis. It is found in the study that a linear combination of the consecutive numerical solutions following the pattern of the nonuniform grid used may improve the accuracy of the numerical solution. We validate our results with several constructive computational experiments.

1. Introduction. The study of analysis on time scales was introduced by Hilger in his Ph.D. dissertation [**6**]. The original motivation of the study was to unify continuous analysis and discrete analysis. A significant amount of time scales related publications can be found nowadays, and some of them had proposed interesting applications of the theory and methods. Recently Eloe et al. [**4, 5**] have initiated the application of the calculus on time scales to questions in adaptive, or variable step, computations. The premise presented here is that a collection of calculus rules, valid in both continuous analysis and discrete analysis, will provide new insight into the qualitative properties of numerical solutions obtained via variable step finite difference schemes.

For the sake of exposition, we address a specific boundary value problem (BVP) for a second order ordinary differential equation of

Received by the editors on April 16, 2003.
2000 AMS *Mathematics Subject Classification.* Primary 34B10, 35K60, 35K65, 65M06, 39A10.
Key words and phrases. Dynamic and differential equations, adaptive method, nonconstant graininess, time scales, delta and nabla derivatives, Green's functions.

the form,

$$x''(t) = f(t), \quad t \in (a, b), \tag{1.1}$$

with homogeneous conjugate or Dirichlet boundary conditions of the form,

$$x(a) = 0, \quad x(b) = 0. \tag{1.2}$$

In [**4, 5**] the authors essentially studied symmetry and anti-symmetry properties of solutions of the BVP (1.1), (1.2). The problems become interesting when one employs what we will tend to call an adaptive grid in a finite difference numerical method. An adaptive grid is a grid with nonconstant step size, or in the terminology of time scale analysis, a grid with nonconstant graininess. So for example in [**5**], the authors show using only elementary calculus methods that if solutions of the BVP (1.1), (1.2) are symmetric about $(a + b)/2$, the numerical solutions obtained by finite difference methods, are not. The numerical solutions do satisfy what the authors call a cross symmetry property with solutions of a companion problem; symmetric numerical solutions, maintaining the original accuracy of the numerical solutions, are constructed as averages of cross-symmetric numerical solutions.

In a completely independent study, Hilger [**7**] developed Fourier analysis on four specific time scales with constant step size and obtained interesting results with respect to symmetry of functions in this environment.

In this paper we continue related studies. The primary contribution of the discussion is that qualitative properties of numerical solutions are obtained as functions of the graininess of the grid. In conventional numerical analysis, it is standard to study the error bounds as functions of the norm of the grid; here the context is different.

We intend that this study be of interest to those working in numerical analysis and scientific computations as well; hence, we do not assume the reader is versed in the theory on time scales. Instead, in the next section, we present a brief introduction to the theory and methods on time scales so that the paper is self-contained. Some of the results proposed in the section as they relate to this particular study are new as well. Section 3 is devoted to the delta and nabla integral relations that

are needed in our further investigations. Several interesting identities are given and proved via Riemann sums on time scales. In Section 4 we concentrate on applications of the methods developed for solving ordinary boundary value problems, which can be viewed as simplified consequences of semi-discretization of the partial differential equations. Finally, we provide a few interesting computational experiments that further illustrate our results.

2. Notes on the numerics. Here we do not assume the reader has background in the theory and methods of time scales. A reader with background in the calculus on time scales may find new relations in the following discussions as well.

A time scale $\mathbf{T}$ is any closed subset of $\mathbf{R}$. Define $\sigma,\ \varrho : \mathbf{T} \to \mathbf{T}$ by

$$\sigma(t) = \inf\{s \in \mathbf{T} : s > t\}, \quad \varrho(t) = \sup\{s \in \mathbf{T} : s < t\}.$$

If $\mathbf{T}$ is bounded above, we define $\inf \varnothing := \max \mathbf{T}$. If $\mathbf{T}$ is bounded below, we define $\sup \varnothing := \min \mathbf{T}$. $t \in \mathbf{T}$ is called left-dense, left-scattered, right-dense, right-scattered if $\varrho(t) = t$, $\varrho(t) < t$, $\sigma(t) = t$, $\sigma(t) > t$, respectively. If $\mathbf{T}$ has a maximal element, say b, define $\mathbf{T}^\kappa = \mathbf{T}$ if b is left-dense and $\mathbf{T}^\kappa = \mathbf{T} \setminus \{b\}$ if b is left-scattered. Define the *graininess* of $\mathbf{T}$ by $\mu : \mathbf{T}^\kappa \to \mathbf{R}^+$, $\mu(t) = \sigma(t) - t$. If $\mathbf{T}$ has a minimal element, say a, define $\mathbf{T}_\kappa = \mathbf{T}$ if a is right-dense and $\mathbf{T}_\kappa = \mathbf{T} \setminus \{a\}$ if a is right-scattered. Define

$$\mathbf{T}_\kappa^\kappa = \mathbf{T}_\kappa \cap \mathbf{T}^\kappa.$$

We say that a function f defined on $\mathbf{T}$ is Δ *differentiable* at $t \in \mathbf{T}$ if for all $\varepsilon > 0$ there is a neighborhood U of t such that for some γ the inequality

$$|f(\sigma(t)) - f(s) - \gamma(\sigma(t) - s)| < \varepsilon|\sigma(t) - s|$$

is true for all $s \in U$, and in this case we write $f^\Delta(t) = \gamma$. We say that a function f defined on $\mathbf{T}$ is ∇ *differentiable* at $t \in \mathbf{T}$ if for all $\varepsilon > 0$ there is a neighborhood V of t such that for some $\hat{\gamma}$ the inequality

$$|f(\varrho(t)) - f(s) - \hat{\gamma}(\varrho(t)) - s)| < \varepsilon|\varrho(t) - s|$$

is true for all $s \in V$, and in this case we write $f^{\nabla}(t) = \hat{\gamma}$. In order to study second order dynamic equations, define inductively $f^{\Delta\nabla} = \left(f^{\Delta}\right)^{\nabla}$, $f^{\nabla\Delta} = \left(f^{\nabla}\right)^{\Delta}$. For the sake of notation, let $f^{\Delta^0} = f^{\nabla^0} = f$ and $\sigma^0(t) = \varrho^0(t) = t$.

Note that, if $\mathbf{T} = \mathbf{R}$, we have for $t \in \mathbf{R}$

$$\sigma(t) = \varrho(t) = t, \quad \mu(t) = 0, \quad f^{\Delta}(t) = f^{\nabla}(t) = f'(t)$$

if $f : \mathbf{R} \to \mathbf{R}$ is a differentiable function, and hence dynamic equations on this time scale are ordinary differential equations. If, on the other hand, $\mathbf{T} = \mathbf{Z}$, then for $t \in \mathbf{Z}$

$$\sigma(t) = t + 1, \quad \varrho(t) = t - 1, \quad \mu(t) = 1, \quad f^{\Delta}(t) = \Delta f(t)$$

if $f : \mathbf{Z} \to \mathbf{R}$ is a sequence where $\Delta f(t) = f(t+1) - f(t)$ is the usual forward difference operator; similarly

$$f^{\nabla}(t) = f(t) - f(t-1) = \Delta f(t-1) = f^{\Delta}(\varrho(t)).$$

We may state

Lemma 2.1. *Let f and g be functions on $\mathbf{T}$, and let $t \in \mathbf{T}^{\kappa}$. Then*:

1. *if f is differentiable at t, then f is continuous at t;*
2. *if t is right-scattered and f is continuous at t, then*

$$f^{\Delta}(t) = \frac{f(\sigma(t)) - f(t)}{\mu(t)};$$

3. *if $f(t)$ exists, then $f(\sigma(t)) = f(t) + \mu(t) f^{\Delta}(t)$;*
4. *if $f^{\Delta}(\varrho(t))$ exists and if t is left-scattered, then*

$$f^{\Delta}(\varrho(t)) = \frac{f(t) - f(\varrho(t))}{\mu(\varrho(t))};$$

5. *if $f^{\Delta}(t)$ exists on $\mathbf{T}^{\kappa}$ and f is invertible on $\mathbf{T}$, then*

$$\left(f^{-1}\right)^{\Delta}(t) = -(f(\sigma(t))^{-1} f^{\Delta}(t) f^{-1}(t))$$

on $\mathbf{T}^{\kappa}$.

Lemma 2.2. *If f and g are differentiable at $t \in \mathbf{T}^{\kappa}$, then*

$$(fg)^{\Delta}(t) = g(\sigma(t))f^{\Delta}(t) + g^{\Delta}(t)f(t);$$
$$(f/g)^{\Delta}(t) = (g(t)f^{\Delta}(t) - g^{\Delta}(t)f(t))/[g(\sigma(t))g(t)],$$

where the quotient rule is valid provided $g(t)g(\sigma(t)) \neq 0$.

Similar properties are valid for the ∇ derivative.

If f has an antiderivative F, i.e., $F^{\Delta} = f$, then we define an integral by $\int_r^s f(t)\Delta t = F(s) - F(r)$. Or if $F^{\nabla} = f$, then $\int_r^s f(t)\nabla t = F(s) - F(r)$. It is known that any continuous function possesses either anti-derivative.

We refer the reader to the authoritative account [**3**] by Bohner and Peterson for a comprehensive development of time scales calculus; we refer the reader to [**1, 2**] for initial developments of the calculus corresponding to the ∇ derivative.

In this particular study, we consider a bounded discrete time scale

$$\mathbf{T} = \{t_i\}, \quad t_i < t_{i+1},$$

where

$$a = \min \mathbf{T}, \quad b = \max \mathbf{T}.$$

In this setting, there is the property that, on $\mathbf{T}_{\kappa}^{\kappa}$,

$$\sigma \circ \varrho = \mathrm{id} \quad \text{and} \quad \varrho \circ \sigma = \mathrm{id}. \tag{2.1}$$

For general time scales, the property (2.1) is equivalent to

$$t \in \mathbf{T} \text{ left-dense} \iff t \text{ right-dense}.$$

Definition 2.1. Let $\mathbf{T}$ be a bounded discrete time scale. If

1. the sign of $\mu^{\Delta}(s)$, $s \in \mathbf{T}$, is fixed, then $\mathbf{T}$ is called a monotone time scale, or a monotone adaptive grid in computations;

2. $\mathbf{T}$ can be split into sub-time scale $\mathbf{T}_1$, $\mathbf{T}_2, \ldots, \mathbf{T}_m$ such that $\mathbf{T}_1 \cup \mathbf{T}_2 \cup \cdots \cup \mathbf{T}_m = \mathbf{T}$, and the sign of $\mu^{\Delta}(s)$ is fixed as $s \in \mathbf{T}_l$,

$l = 1, 2, \ldots, m$, then $\mathbf{T}$ is called a piecewise monotone time scale, or a piecewise monotone adaptive grid in computations.

Remark 2.1. The graininess is not differentiable in general. To see this, we consider the bounded time scale

$$\mathbf{T} = \left\{ \pm 2^{-n} \;\middle|\; n \in \mathbf{Z} \right\} \cup \{0\}.$$

We only need to consider the case with Δ derivative since discussions with ∇ derivative are similar.

Case I. Let $s_n = -2^{-n},\ n \geq 0$. We have $\sigma(s_n) = -2^{-n-1}$, $\sigma^2(s_n) = -2^{-n-2}$ and $\mu(s_n) = 2^{-n-1},\ n \geq 0$. Therefore

$$\begin{aligned} \mu^{\Delta}(s_n) &= \frac{\mu(s_n) - \mu(\sigma(s_n))}{s_n - \sigma(s_n)} \\ &= \frac{\left(-2^{-n-2} + 2^{-n-1}\right) - \left(-2^{-n-1} + 2^{-n}\right)}{-2^{-n-1} + 2^{-n}} = -\frac{1}{2}, \quad n \geq 0. \end{aligned}$$

Case II. Let $t_n = 2^{-n},\ n \geq 0$. We have $\sigma(t_n) = 2^{-n+1}$, $\sigma^2(t_n) = 2^{-n+2}$ and $\mu(t_n) = 2^{-n},\ n \geq 2$. Therefore

$$\begin{aligned} \mu^{\Delta}(t_n) &= \frac{\mu(t_n) - \mu(\sigma(t_n))}{t_n - \sigma(t_n)} \\ &= \frac{\left(2^{-n+2} - 2^{-n+1}\right) - \left(2^{-n+1} - 2^{-n}\right)}{2^{-n+1} - 2^{-n}} = 1, \quad n \geq 2. \end{aligned}$$

Case III. Let $t = 0$. We may let $n \to \infty$ in previous cases and consider the limits. However, on the other hand, it is not difficult to see that the point is right-dense and left-dense. Thus, for $s \in \mathbf{T}$, $s \neq t$ we have

$$\frac{\mu(t) - \mu(\sigma(s))}{t - \sigma(s)} = \frac{0 - [\sigma(\sigma(s)) - \sigma(s)]}{0 - \sigma(s)} = \frac{\sigma(\sigma(s))}{\sigma(s)} - 1.$$

The sequence $s_n = -2^{-n}$ is increasing convergent to 0, and

$$\lim_{n \to \infty} \frac{\sigma(\sigma(s_n))}{\sigma(s_n)} = \lim_{n \to \infty} \frac{-2^{-(n+2)}}{-2^{-(n+1)}} = \frac{1}{2}.$$

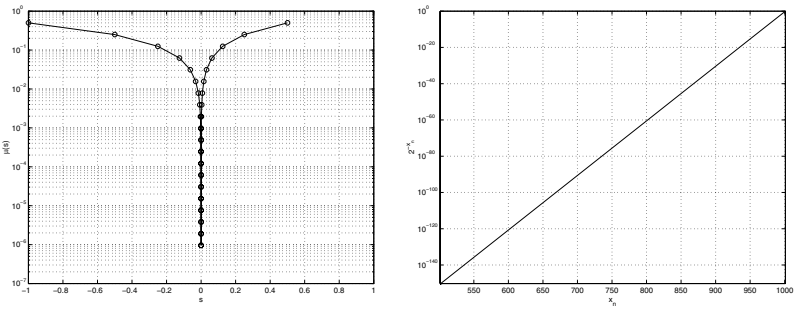

FIGURE 2.1. The graininess function $\mu(s)$, $s \in \mathbf{T} \setminus \{0\}$. Forty-one points are used.

on the other hand, the sequence $t_n = 2^{-n}$ is decreasing convergent to 0, and

$$\lim_{n\to\infty} \frac{\sigma(\sigma(t_n))}{\sigma(t_n)} = \lim_{n\to\infty} \frac{2^{-(n-2)}}{2^{-(n-1)}} = 2.$$

So the righthanded and lefthanded limits in the definition of μ^{Δ} do not coincide. This is consistent with our results by taking the limits in cases 1 and 2. Therefore μ is not differentiable at 0. In fact, for $s < 0$, the graininess $\mu(s)$ decreases at a constant rate -1/2, while for $s > 0$, the graininess $\mu(s)$ increases at a different constant rate 1. These imply that $\mu^{\Delta\Delta}(s) = 0$ for $s \neq 0$ which indicates a piecewise monotone adaptive grid satisfying ideal smoothness constraints

$$\min\{\mu(s_{n-1}), \mu(s_{n+1})\} \geq \frac{1}{2}\,\mu(s_n), \quad \max\{\mu(s_{n-1}), \mu(s_{n+1})\} \leq 2\mu(s_n).$$

The time scale involved is also symmetric with respect to 0, To see more precisely the structure of the graininess function $\mu(s)$, we plot it over $\mathbf{T} \setminus \{0\}$ in Figure 2.1. A logarithmic scale is used to show more clearly the details.

In our particular setting, we consider operators

$$f^{\Delta}(t) = \frac{f(\sigma(t)) - f(t)}{\mu(t)}$$

and

$$f^{\nabla}(t) = \frac{f(t) - f(\varrho(t))}{\varrho(t)} = f^{\Delta\varrho}(t). \tag{2.2}$$

The adjoint operator of Δ is $-\nabla$; this means that

$$\int_a^b f^{\Delta}(t) \cdot g(t) \Delta t = \int_a^b f(t) \cdot \left[-g^{\nabla}(t)\right] \Delta t$$

for the Dirichlet or conjugate boundary conditions we consider. To see this, integrate the product rule formula given in Lemma 2.2 and apply (2.2).

Lemma 2.3. *The following identities hold*:

$$\begin{aligned} \mu^{\Delta\varrho} &= \frac{\mu}{\mu^{\varrho}} - 1; \\ \mu^{\varrho\Delta} &= 1 - \frac{\mu^{\varrho}}{\mu}; \\ \mu^{\varrho} \cdot \mu^{\Delta\varrho} &= \mu \cdot \mu^{\varrho\Delta}; \\ \left[1+\mu^{\Delta\varrho}\right] \cdot \left[1-\mu^{\varrho\Delta}\right] &= 1. \end{aligned} \tag{2.3}$$

Proof. The proof consists of thoroughly expressing the expressions for $\mu^{\Delta\varrho}$ and $\mu^{\varrho\Delta}$

$$\begin{aligned} \mu^{\Delta\varrho}(t) &= \left[\frac{\mu(\sigma(t)) - \mu(t)}{\sigma(t) - t}\right]^{\varrho} = \frac{\mu(t) - \mu^{\varrho}(t)}{\mu^{\varrho}(t)} = \frac{\mu(t)}{\mu^{\varrho}(t)} - 1, \\ \mu^{\varrho\Delta}(t) &= \frac{\mu^{\varrho}(\sigma(t)) - \mu^{\varrho}(t)}{\sigma(t) - t} = \frac{\mu(t) - \mu^{\varrho}(t)}{\mu(t)} = 1 - \frac{\mu^{\varrho}(t)}{\mu(t)}. \end{aligned}$$

□

Lemma 2.4. *We further have the following identities*:

$$f^{\Delta\varrho} = \frac{\mu}{\mu^{\varrho}} \cdot f^{\varrho\Delta} = \left[1 + \mu^{\Delta\varrho}\right] \cdot f^{\varrho\Delta} = \left[1 - \mu^{\varrho\Delta}\right]^{-1} \cdot f^{\varrho\Delta}; \tag{2.4}$$

$$f^{\Delta\nabla} = \frac{\mu}{\mu^{\varrho}} \cdot f^{\nabla\Delta} = \left[1 + \mu^{\Delta\varrho}\right] \cdot f^{\nabla\Delta} = \left[1 - \mu^{\varrho\Delta}\right]^{-1} \cdot f^{\nabla\Delta}; \tag{2.5}$$

$$\mu^{\varrho} f^{\Delta\varrho} + \mu f^{\varrho\Delta} = 2 \cdot \left(f - f^{\varrho}\right); \tag{2.6}$$

$$\mu^{\varrho} f^{\Delta\nabla} + \mu f^{\nabla\Delta} = 2 \cdot \left(f^{\Delta} - f^{\nabla}\right). \tag{2.7}$$

Proof. In order to see (2.4) or (2.6), express the relevant expressions again

$$f^{\Delta\varrho}(t) = \left[\frac{f(\sigma(t)) - f(t)}{\sigma(t) - t}\right]^{\varrho} = \frac{f(t) - f^{\varrho}(t)}{\mu^{\varrho}(t)},$$
$$f^{\varrho\Delta}(t) = \frac{f^{\varrho}(\sigma(t)) - f^{\varrho}(t)}{\sigma(t) - t} = \frac{f(t) - f^{\varrho}(t)}{\mu(t)}.$$

In order to check the equations in (2.5) or (2.7), insert f^{Δ} for f, and observe

$$f^{\Delta\nabla}(t) = \left(f^{\Delta}\right)^{\Delta\varrho}(t) \quad \text{and} \quad f^{\nabla\Delta}(t) = \left(f^{\Delta}\right)^{\varrho\Delta}(t). \qquad \square$$

Remark 2.2. Let $\mathbf{T}$ be monotone and $\mu(t) \neq 0$, $t \in \mathbf{T}$. Then the following relations hold:

$$\frac{\mu}{\mu^{\varrho}} \begin{cases} > 1 & \text{if } \mathbf{T} \text{ is monotonically increasing,} \\ < 1 & \text{if } \mathbf{T} \text{ is monotonically decreasing,} \\ = 1 & \text{if } \mathbf{T} \text{ has a constant graininess.} \end{cases}$$

In practical computations, $\mu^{\varrho} \ll \mu$ may cause a substantial increase of the numerical error. Therefore the situation must be avoided. This leads to the basic smoothness constraint for adaptive computations:

$$m\mu^{\varrho} \leq \mu \leq M\mu^{\sigma},$$

where m and M are positive constants.

3. Delta and nabla integral relations. We develop briefly some new integral relations for the delta and nabla integrals. The concepts are elementary; it is the calculus notation that makes observations so apparent. $\mathbf{T} = \cup_{i=0}^{n} t_i$ where

$$a = t_0 < t_1 < \cdots\cdots t_{n-1} < t_n = b.$$

Definition 3.1. The corresponding integrals for the delta and the nabla derivative are [**3**]:

$$\int_a^b f(t)\Delta t = \sum_{i=0}^{n-1} \mu(t_i) f(t_i) = \sum_{i=1}^{n} \mu^{\varrho}(t_i) f^{\varrho}(t_i);$$
$$\int_a^b f(t)\,\nabla t = \sum_{i=0}^{n-1} \mu(t_i) f^{\sigma}(t_i) = \sum_{i=1}^{n} \mu^{\varrho}(t_i) f(t_i).$$

Remark 3.1. In this setting each integral represents a Riemann sum; the delta integral is the Riemann sum in which the intermediate point is always chosen as the left end point of the appropriate subinterval; the nabla integral is the Riemann sum in which the intermediate point is always chosen as the right end point of the appropriate subinterval.

We compare the two integrals

$$\begin{aligned}
\int_a^b f(t)\,\nabla t - \int_a^b f(t)\Delta t &= \sum_{i=0}^{n-1} \mu(t_i)\cdot\left(f^{\sigma}(t_i) - f(t_i)\right) \\
&= \sum_{i=0}^{n-1} \mu(t_i)\cdot\left(\mu(t_i)\cdot f^{\Delta}(t_i)\right) = \int_a^b \mu(t)\cdot f^{\Delta}(t)\Delta t \\
&= \int_a^b \mu^{\sigma\varrho}(t)\cdot f^{\Delta}(t)\Delta t \\
&\qquad \text{(partial integration left)} \\
&= \mu(b)\cdot f(b) - \mu(a)\cdot f(a) - \int_a^b \mu^{\Delta}(t)\cdot f^{\sigma}(t)\Delta t \\
&\qquad \text{(partial integration right)} \\
&= \mu^{\varrho}(b)\cdot f(b) - \mu^{\varrho}(a)\cdot f(a) - \int_a^b \mu^{\varrho\Delta}(t)\cdot f(t)\Delta t.
\end{aligned}$$

A simple consequence of this identity is the following

Lemma 3.1. *Let a function $f : \mathbf{T} \to \mathbf{R}$ be given on a time scale $\mathbf{T}$, such that on $[a, b] \subseteq \mathbf{T}$*

$$f(a) = f(b) = 0 \quad \textit{and} \quad f(t) \geq 0 \quad \textit{for } t \in [a, b].$$

Then

$$\mu \text{ increasing} \implies \int_a^b f(t)\Delta t \geq \int_a^b f(t)\,\nabla t$$

$$\mu \text{ decreasing} \implies \int_a^b f(t)\,\nabla t \geq \int_a^b f(t)\Delta t.$$

Lemma 3.2. *We have the following identity*:

$$\int_a^{\varrho(b)} \mu^{\Delta\varrho}(t) f(t)\,\nabla t = \int_{\sigma(a)}^b \mu^{\varrho\Delta}(t) f(t)\Delta t \tag{3.1}$$

Proof. Straightforward computations yield

$$\int_a^{\varrho(b)} \mu^{\Delta\varrho}(t) f(t)\,\nabla t = \sum_{i=1}^{n-1} \mu^{\varrho}(t_i)\mu^{\Delta\varrho}(t_i) f(t_i)$$

$$\int_{\sigma(a)}^b \mu^{\varrho\Delta}(t) f(t)\Delta t = \sum_{i=1}^{n-1} \mu(t_i)\mu^{\varrho\Delta}(t_i) f(t_i)$$

Now compare with identity (2.3). □

4. Numerical solutions of BVPs. We now consider the numerical solution of BVP (1.1), (1.2). Our intention here is to show that the time scale calculus formulas derived above or elsewhere give new and useful insight to qualitative features of numerical solutions. A standard method to construct a numerical solution of the BVP (1.1), (1.2) is to solve the BVP

$$w^{\nabla\Delta}(t) = f(t), \quad t \in \mathbf{T}_\kappa^\kappa, \quad w(a) = 0,\ w(b) = 0,$$

or to solve the BVP

$$v^{\Delta\nabla}(t) = f(t), \quad t \in \mathbf{T}_\kappa^\kappa, \quad v(a) = 0,\ v(b) = 0.$$

Is there a tendency to take care which BVP one chooses to solve? What insight may time scales analysis provide into the choice of a

numerical method? Note that

(4.1)
$$\begin{aligned}(w-v)^{\Delta\nabla}(t) &= w^{\Delta\nabla}(t) - v^{\Delta\nabla}(t) = [1+\mu^{\Delta\varrho}]\cdot w^{\nabla\Delta}(t) - v^{\Delta\nabla}(t)\\ &= [1+\mu^{\Delta\varrho}]\cdot f(t) - f(t) = \mu^{\Delta\varrho} f(t).\end{aligned}$$

This implies [**3, 5**]

$$(w-v)(t) = \int_a^{\varrho(b)} H(t,s)\cdot\left(\mu^{\Delta\varrho} f\right)(s)\,\nabla s,$$

where the Green's function is defined as

$$H(t,s) = \begin{cases} (t-a)\cdot(s-b)/(b-a) & \text{if } t < s,\\ (s-a)\cdot(t-b)/(b-a) & \text{if } t \geq s.\end{cases}$$

On the other hand we have

(4.2)
$$\begin{aligned}(w-v)^{\nabla\Delta}(t) &= w^{\nabla\Delta}(t) - v^{\nabla\Delta}(t) = w^{\nabla\Delta}(t) - [1-\mu^{\varrho\Delta}]\cdot v^{\Delta\nabla}(t)\\ &= f(t) - [1-\mu^{\varrho\Delta}]\cdot f(t) = \mu^{\varrho\Delta} f(t).\end{aligned}$$

Now this implies [**3, 5**]

$$(w-v)(t) = \int_{\sigma(a)}^{b} H(t,s)\cdot\left(\mu^{\varrho\Delta} f\right)(s)\Delta\, s.$$

We did not state such properties with respect to integration in Section 3, but properties we expect, such as

$$g \geq 0 \Longrightarrow \int_{\mathbf{T}} g\Delta s \geq 0$$

are valid. Note that $H(t,s) \leq 0$ on $\mathbf{T}^2$. We have the following simple consequence.

Lemma 4.1. *Let* $\mathbf{T}$ *be monotone.*

1. *If* $f \in C[a,b]$ *is nonpositive* (*so that the solution,* x *of* (1.1), (1.2) *is concave*). *Then*

$$\begin{aligned} \mu \text{ increasing} &\implies w \geq v, \\ \mu \text{ decreasing} &\implies w \leq v. \end{aligned}$$

2. *If* $f \in C[a,b]$ *is nonnegative. Then*

$$\begin{aligned} \mu \text{ increasing} &\implies w \leq v, \\ \mu \text{ decreasing} &\implies w \geq v. \end{aligned}$$

We close this investigation by considering linear combinations of v and w as a natural numerical approximation to the solution of the BVP, (1.1), (1.2). In [**4**] and [**5**] the authors appealed to shape features, symmetry or anti-symmetry about $(a+b)/2$ to support the claim that the average $(w+v)/2$ is the natural numerical solution of the BVP, (1.1), (1.2). Here, with the help of the calculus rules developed above, we appeal to more Taylor series expansions related to truncation error.

Remark 4.1. Let x denote the solution of the BVP, (1.1), (1.2). According to the definition of the dynamic derivatives, we have

$$x^{\nabla\Delta}(t) = \frac{x(\sigma(t)) - x(t)}{\mu^2(t)} - \frac{x(t) - x(\varrho(t))}{\mu(t)\mu(\varrho(t))}.$$

Assume for convenience that x is three times differentiable and expand $x\circ\sigma$, $x\circ\varrho$ about t. Note that the time scale $\mathbf{T}$ can be viewed as a set superimposed on an interval. A straightforward calculation gives

$$\begin{aligned} x^{\nabla\Delta}(t) &= \frac{1}{2}\left(1 + \frac{\mu(\varrho(t))}{\mu(t)}\right)x''(t) + \frac{\mu(t)}{3!}\,x'''(t) - \frac{\mu^2(\varrho(t))}{3!\mu(t)}\,x'''(t) \\ &\quad + \mathrm{O}(\mu^2(t)) + \mathrm{O}\left(\frac{\mu^3(\varrho(t))}{\mu(t)}\right) \\ &= \frac{1}{2}\left(1 + \frac{\mu(\varrho(t))}{\mu(t)}\right)f(t) + \frac{1}{3!}\left[\mu(t) - \frac{\mu^2(\varrho(t))}{\mu(t)}\,\mathbf{R}\right]x'''(t) \\ &\quad + \mathrm{O}(\mu^2(t)\mathbf{R}) + \mathrm{O}\left(\frac{\mu^3(\varrho(t))}{\mu(t)}\right). \end{aligned} \tag{4.3}$$

Similarly,

(4.4)

$$\begin{aligned} x^{\Delta\nabla}(t) &= \frac{1}{2}\left(1+\frac{\mu(t)}{\mu(\varrho(t))}\right)x''(t) - \frac{\mu(\varrho(t))}{3!}\,x'''(t) + \frac{\mu^2(t)}{3!\mu(\varrho(t))}\,x'''(t) \\ &\quad + \mathrm{O}(\mu^2(\varrho(t))) + \mathrm{O}\left(\frac{\mu^3(t)}{\mu(\varrho(t))}\right) \\ &= \frac{1}{2}\left(1+\frac{\mu(t)}{\mu(\varrho(t))}\right)f(t) - \frac{1}{3!}\left[\mu(\varrho(t)) - \frac{\mu^2(t)}{\mu(\varrho(t))}\right]x'''(t) \\ &\quad + \mathrm{O}(\mu^2(\varrho(t))) + \mathrm{O}\left(\frac{\mu^3(t)}{\mu(\varrho(t))}\right). \end{aligned}$$

We may notice that when $\mathbf{T}$ is uniform, (4.3), (4.4) reduce to the following:

$$x^{\nabla\Delta}(t) = f(t) + \mathrm{O}(\mu^2(t))$$

which is consistent with the central difference scheme [**8**].

Formulae (4.3), (4.4) further suggest the following new schemes for approximating (1.1), (1.2):

$$\tilde{w}^{\Delta\nabla}(t) = \frac{1}{2}\left(1+\frac{\mu(t)}{\mu(\varrho(t))}\right)f(t), \quad t \in \mathbf{T}_\kappa^\kappa, \tag{4.5}$$

$$\tilde{v}^{\nabla\Delta}(t) = \frac{1}{2}\left(1+\frac{\mu(\varrho(t))}{\mu(t)}\right)f(t), \quad t \in \mathbf{T}_\kappa^\kappa, \tag{4.6}$$

together with the homogeneous conjugate or Dirichlet boundary conditions. The method (4.5) may offer a better accuracy on any monotonically decreasing $\mathbf{T}$, while (4.6) should give a better result if $\mathbf{T}$ is monotonically increasing due to expansions in (4.3), (4.4).

Remark 4.2. Set

$$\eta(t) = \frac{v(t)+w(t)}{2},\ \phi(t) = \frac{v(t)+\tilde{w}(t)}{2},\ \psi(t) = \frac{\tilde{v}(t)+w(t)}{2}, \quad t \in \mathbf{T}_\kappa^\kappa.$$

Recall (4.1), (4.2). We obtain from (4.5), (4.6) and the above equations the combined consecutive algorithms via graininess functions:

$$\eta^{\nabla\Delta}(t) = \frac{1}{2}\,(2 - \mu^{\varrho\Delta})f(t), \tag{4.7}$$

$$\eta^{\Delta\nabla}(t) = \frac{1}{2}\,(2 + \mu^{\Delta\varrho})f(t), \tag{4.8}$$

$$\phi^{\nabla\Delta}(t) = \frac{1}{4}\left(3 + \frac{\mu(\varrho(t))}{\mu(t)}\right)f(t), \tag{4.9}$$

$$\psi^{\Delta\nabla}(t) = \frac{1}{4}\left(3 + \frac{\mu(t)}{\mu(\varrho(t))}\right)f(t) \tag{4.10}$$

for $t \in \mathbf{T}_{\kappa}^{\kappa}$.

Numerical experiments. Let

$$\mathbf{T} = \{0,\ 7/50,\ 13/50,\ 9/25,\ 11/25,\ 1/2,\ 14/25,\ 16/25,\ 37/50,\ 43/50,\ 1\}$$

be the time scale considered. Therefore $\mathbf{T}$ is a superimposed grid on $[0,\ 1]$. It is easy to see that $\mathbf{T}$ is piecewise monotone, and is symmetric with respect to the centerpoint $t = 1/2$. Consider the following dynamic BVPs on the time scale $\mathbf{T}$:

$$\begin{aligned}
v^{\Delta\nabla} &= -\sin t - \cos t,\ v(0) = v(1) = 0,\\
w^{\nabla\Delta} &= -\sin t - \cos t,\ w(0) = w(1) = 0,\\
\tilde{w}^{\Delta\nabla} &= -\frac{1}{2}\left(1 + \frac{\mu(t)}{\mu(\varrho(t))}\right)(\sin t + \cos t),\ \tilde{v}(0) = \tilde{v}(1) = 0,\\
\tilde{v}^{\nabla\Delta} &= -\frac{1}{2}\left(1 + \frac{\mu(\varrho(t))}{\mu(t)}\right)(\sin t + \cos t),\ \tilde{w}(0) = \tilde{w}(1) = 0.
\end{aligned}$$

In scientific computations, the above equations can be viewed as different finite difference approximations to the differential equation boundary value problem, $x'' = -\sin t - \cos t$, $0 < t < 1$; $x(0) = x(1) = 0$, which possesses the exact solution

$$x(t) = -1 + (1 - \sin 1 - \cos 1)\,t + \sin t + \cos t, \quad 0 \le t \le 1.$$

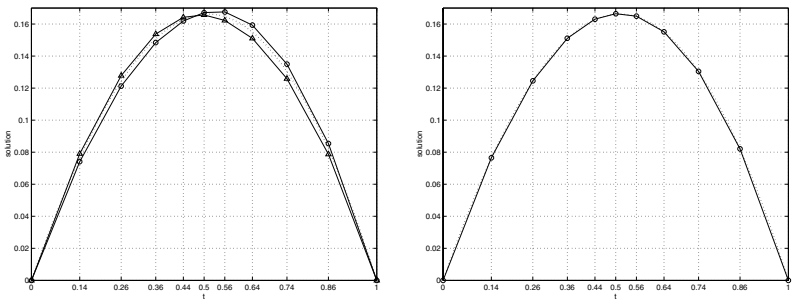

FIGURE 4.1. Solutions of the dynamic equation BVPs and the solution of the corresponding differential equation problem. LEFT: Circled curve is for v, and triangulated curve is for w. RIGHT: Circled curve is for η. Dotted curves are for the true solution x.

In Figure 4.1, we show the numerical solutions v, w and η along with the exact solution x. It is interesting to observe that v and w switch their positions as upper and lower solutions at approximately $t = 0.5$, and the combined solution η indicates a much better approximation to x. The latter will be verified by the relative error analysis in Figure 4.3. Figure 4.2 is for the numerical solutions $\tilde{v}$, $\tilde{w}$ and $\tilde{\eta} = l(\tilde{v}+\tilde{w}\mathbf{R})/2$. The numerical solutions $\tilde{v}$, $\tilde{w}$ and $\tilde{\eta}$ again demonstrate similar properties as that in Figure 4.1. In Figure 4.3, we plot out relative error profiles of the numerical solutions $v, w, \eta, \tilde{v}, \tilde{w}$ and $\tilde{\eta}$, respectively. It is found that the combined solutions $\eta, \tilde{\eta}$ perform much better than any of the ancestor solutions constructed. In particular in the case for η, the maximal relative error appears at $t = 0.14$ is only $0.003 = 0.03\%$ even when large step sizes such as $h = \max \mu = 0.14$ are employed.

We display the numerical solutions ϕ and ψ in Figure 4.4. Their relative errors are also given in the figure. It is noticed that the functions behave similar to the pair of single numerical solutions but provide much sharper approximations to the true solution x. We finally compare relative errors of η and $\tilde{\eta}$ generated via the combined consecutive schemes (4.7)–(4.10) in Figures 4.5, respectively. In this particular experiment, the solution η performs better than $\tilde{\eta}$, possibly due to its relatively simple algorithm, and for less truncation error involved while approximating the differential equation (1.1). However, in the consideration of relatively large step sizes such as $h = \max \mu =$

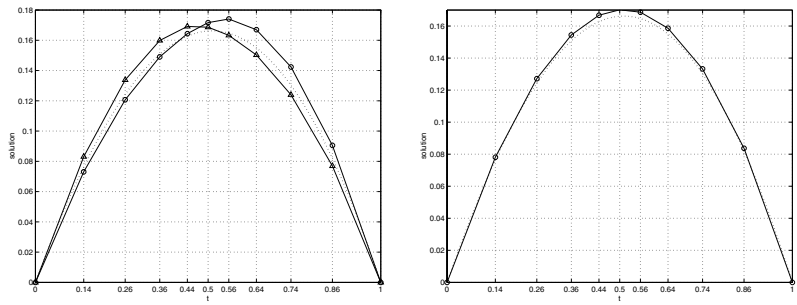

FIGURE 4.2. Solutions of the dynamic equation BVPs and the solution of the corresponding differential equation problem. LEFT: Circled curve is for $\tilde{v}$, and triangulated curve is for $\tilde{w}$. RIGHT: Circled curve is for η. Dotted curves are for the true solution x.

0.14 are used, both η and $\tilde{\eta}$ provide satisfactory results for achieving less than $0.025 = 2.5\%$ of the relative error. The consecutively combined numerical solution demonstrate a superior quality in approximations.

Trigonometric types function f used in the experiments have a general meaning in applications where periodic forcing terms are significant. Readers are referred to our previous publications [**4, 5**] for detailed

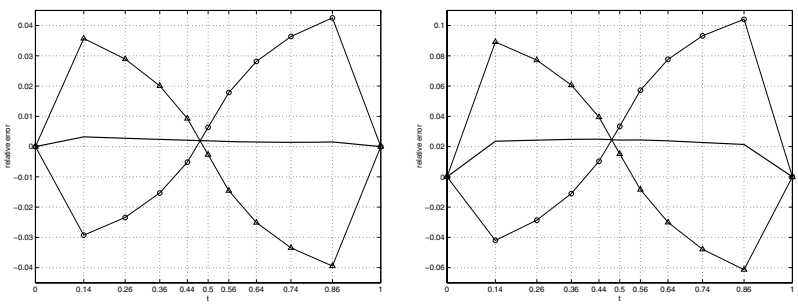

FIGURE 4.3. Relative error of the numerical solutions. LEFT: Circled curve is for v, and triangulated curve is for w. The solid curve is for η. RIGHT: Circled curve is for $\tilde{v}$. and triangulated curve is for $\tilde{w}$. The solid curve is for $\tilde{\eta}$. Note that the error for η or $\tilde{\eta}$ is significantly less than that of their counterparts.

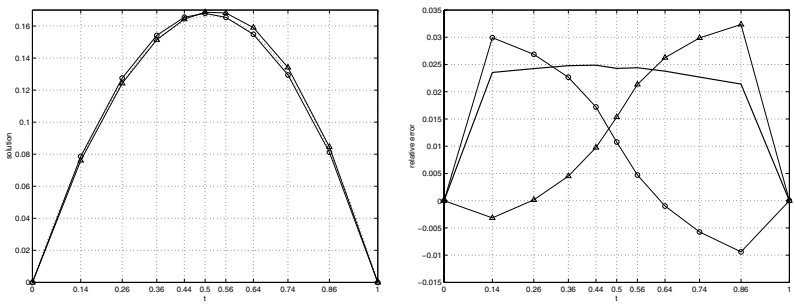

FIGURE 4.4. LEFT: Numerical solution: circled curve is for ϕ, triangulated curve is for ψ. Dotted curve is for the true solution x. RIGHT: Relative error: circled curve is for ϕ, triangulated curve is for ψ, and the solid curve is for $\tilde{\eta}$. The magnitudes of the latter is less than the formers though they are at approximately the same level.

discussions and numerical examples in which polynomials functions are used as the right-hand side functions of the two-point dynamic boundary value problems.

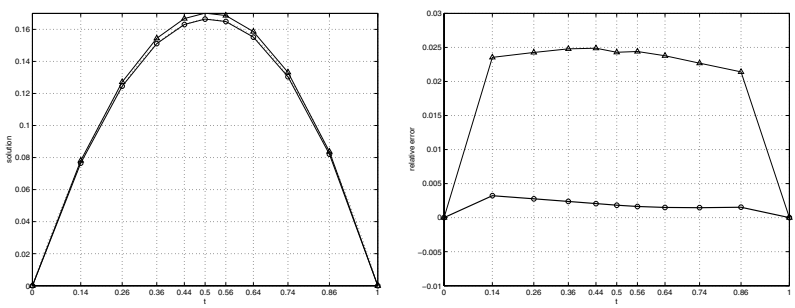

FIGURE 4.5. Comparisons of the combined numerical solutions. LEFT: Numerical solutions: circled curve is for η, triangulated curve is for $\tilde{\eta}$. Dotted curve is for the true solution x. RIGHT: Relative error: circled curve is for η, triangulated curve is for $\tilde{\eta}$.

REFERENCES

1. D. Anderson, J. Bullock, L. Erbe, A. Peterson and H. Tran, *Nabla dynamic equations on time scales*, PanAmerican Math. J. **13** (2003), 1–47.

2. F. Atici and G.Sh. Guseinov, *On Green's functions and positive solutions for boundary value problems on time scales*, J. Comput. Appl. Math. **141** (2002), 75–99.

3. M. Bohner and A.C. Peterson, *Dynamic equations on time scales–An introduction with applications*, Birkhäuser, Boston, 2001.

4. P.W. Eloe and Q. Sheng, *A continuation of the discussion on cross symmetry of solutions*, Dynamic Systems Appl. **12** (2003), 99–114.

5. P.W. Eloe, Q. Sheng and J. Henderson, *Notes on crossed symmetry solutions of the two-point boundary value problems on time scales*, J. Differential Equations Appl. **9** (2003), 29–48.

6. S. Hilger, *Ein Maßkettenkalkül mit Anwendung auf Zentrumsmannigfaltigkeiten*, Ph.D. Thesis, Universität Würzburg, Germany, 1988.

7. ———, *An application of calculus on measure chains to Fourier theory and Heisenberg's uncertainty principle*, J. Differential Equations Appl. **8** (2003), 897–936.

8. H.B. Keller, *Numerical methods for two-point boundary-value problems*, Dover Publ., New York, 1992.

Department of Mathematics, University of Dayton, Dayton, OH 45469-2316
E-mail address: Paul.Eloe@notes.udayton.edu

Katholische Universität Eichstätt, D-85071 Eichstätt, Germany
E-mail address: Stefan.Hilger@ku-eichstaett.de

Department of Mathematics, University of Dayton, Dayton, OH 45469-2316
E-mail address: Qin.Sheng@notes.udayton.edu

Current address: Department of Mathematics, Baylor University, Waco, TX 76798-7328
E-mail address: Qin_Sheng@baylor.edu